Density matrix renormalization group based downfolding of the three-band Hubbard model: Importance of density-assisted hopping

Shengtao Jiang (□□□), Douglas J. Scalapino, and Steven R. White

Phys. Rev. B **108**, L161111 — Published 24 October 2023

DOI: 10.1103/PhysRevB.108.L161111

Density-matrix-renormalization-group-based downfolding of the three-band Hubbard model: the importance of density-assisted hopping

Shengtao Jiang (蒋晟韬),[1,*] Douglas J. Scalapino,[2] and Steven R. White[1]

[1] *Department of Physics and Astronomy, University of California, Irvine, California 92697, USA*

[2] *Department of Physics, University of California, Santa Barbara, California 93106, USA*

(Dated: October 4, 2023)

Typical Wannier-function downfolding starts with a mean-field or density functional set of bands to construct the Wannier functions. Here we carry out a controlled approach, using DMRG-computed natural orbital bands, to downfold the three-band Hubbard model to an effective single band model. A sharp drop-off in the natural orbital occupancy at the edge of the first band provides a clear justification for a single-band model. Constructing Wannier functions from the first band, we compute all possible two-particle terms and retain those with significant magnitude. The resulting single-band model includes two-site density-assisted hopping terms with $t_n \sim 0.6t$. These terms lead to a reduction of the ratio $U/t_{\rm eff}$, and are important in capturing the doping-asymmetric carrier mobility, as well as in enhancing the pairing in a single-band model for the hole-doped cuprates.

Introduction.— What is the minimal model that captures the important physics of the high-temperature cuprate superconductors? This has been a central question ever since the discovery of the cuprates. It has been argued that the single-band Hubbard and t-J models, in their simplest forms, are sufficient to describe the physics of high T_c superconductivity. Unexpectedly, recent numerical simulations find that superconductivity in the ground state of these single-band models appears to be quite delicate. For example, in the pure Hubbard and t-J models ($t', t'' = 0$), superconductivity is found to be absent [1, 2]. While the presence of a $t' > 0$ can induce superconductivity [2–7], this corresponds to electron doping and the question regarding the presence of hole-doped superconductivity ($t' < 0$) is not completely resolved [2, 4, 6–8]. The greatest delicacy appears to be associated with the superconductivity; other aspects of the models, including antiferromagnetism(AFM) as well as intertwined spin and charge order, appear to be in qualitative agreement with the cuprates [2, 9–15].

This subtleness of pairing in the single-band models calls for a re-examination of the downfolding process used to derive them, since modest errors could have significant effects. This downfolding is a two-step process, where first one constructs from density functional methods the intermediate-level three-band Hubbard (or Emery) model [16], which includes Cu $d_{x^2-y^2}$, O p_x and O p_y orbitals. Since the three-band model is closer to an all-electron Hamiltonian of the cuprates, one expects it to be more reliable than a one-band model—but also more difficult to simulate. There is evidence that the three-band model captures various aspects of the cuprates, particularly magnetic and charge density wave properties [17–24], with greater uncertainty about the pairing properties. To downfold to a single band model, Zhang and Rice argued that holes on oxygen sites bind to holes on copper sites to form local singlets [25]. The Zhang-Rice singlet picture has gained support from experiments [26–28] as well as calculations [18, 19, 29, 30], and motivated studies of various single-band Hubbard [7, 31–50] and t-J models [3, 5, 11, 51–58].

Here we demonstrate an alternative way to downfold the three-band Hubbard model based on a density-matrix renormalization group (DMRG) [59] construction of Cu-centered Wannier functions. The general idea of constructing effective models using *ab initio* calculations has been explored in various contexts [60–64]. Our approach uses DMRG to compute the natural orbitals of the three-band model, and from those construct Wannier functions, similar to a recent work that downfolds hydrogen chains into Hubbard-like models [65]. The resulting single-band model includes additional two-site density-assisted hopping terms t_n whose magnitude is comparable to t. On a mean-field level, these new terms simply reduce the ratio $U/t_{\rm eff}$, with $t_{\rm eff} = t + t_n\langle n\rangle$, where $\langle n\rangle$ is the average number of holes per CuO_2 unit cell. However, beyond mean-field, the t_n terms capture the doping-asymmetric carrier mobility, and, as revealed by a measurement of the superconducting phase stiffness, further enhance the pairing in the hole-doped single-band model.

The three-band model.—We present the lattice structure and the terms in the three-band Hubbard model in Fig. 1(a). Each CuO_2 unit cell consists of three orbitals: Cu $d_{x^2-y^2}$, O p_x and O p_y. We study clusters with cylindrical boundary conditions. For an L_x by L_y cylinder, there are $N_{\rm Cu}{=}L_xL_y$ Cu sites and $N_{\rm O}{=}(2L_x+1)L_y$ O sites. In the undoped insulator at half-filling, there is one hole per unit cell, and the model is written in the hole picture with $d^\dagger_{i\sigma}$ or $p^\dagger_{j\sigma}$ creating a hole with spin σ on a Cu site i or O site j. Hole doping corresponds to $\langle n\rangle > 1$ while electron doping corresponds to $\langle n\rangle < 1$. The three-band Hamiltonian is:

$$H^{TB} = -t_{pd}\sum_{\langle ij\rangle\sigma}(d^\dagger_{i\sigma}p_{j\sigma} + h.c.) - t_{pp}\sum_{\langle\langle ij\rangle\rangle\sigma}(p^\dagger_{i\sigma}p_{j\sigma} + h.c.) + U_d\sum_i n^d_{i\uparrow}n^d_{i\downarrow} + U_p\sum_i n^p_{i\uparrow}n^p_{i\downarrow} + \Delta_{pd}\sum_{i\sigma}p^\dagger_{i\sigma}p_{i\sigma} \quad (1)$$

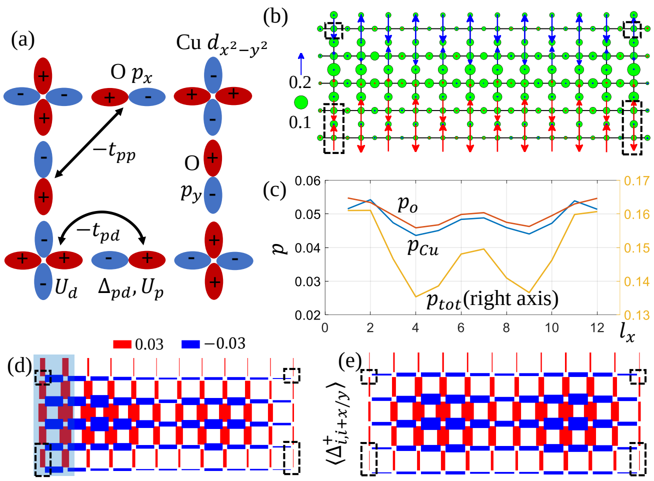

FIG. 1. (a): The three-band Hubbard model and our phase convention for the orbital basis. (b): Charge and spin structure on a 12×5 cylinder at a hole doping ∼ 0.15. The length of the arrows and the diameter of the circles represent $\langle S^z\rangle$ and local doping, respectively. The spins are colored to indicate different AFM domains. There are weak magnetic pinning fields applied on the boundary sites in the dotted boxes. (c): Average orbital-resolved local doping $p_{\mathrm{Cu/O}}$ along the length of the cylinder with $p_{\mathrm{tot}}{=}p_{\mathrm{Cu}}+2p_{\mathrm{O}}$ (d) and (e): Pairing order $\langle\Delta^{\dagger}_{ij}+\Delta_{ij}\rangle$ between neighboring Cu sites i and j. The thickness/color of the bond indicates the magnitude/sign of the pairing. The pairing orders away from the edges are similar for (d) which has pairfields applied on the shaded left edge and (e) which spontaneously breaks symmetry.

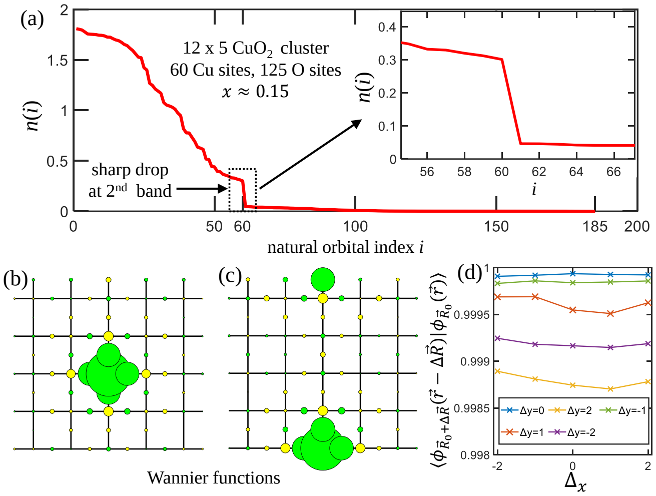

FIG. 2. At a hole doping of 0.15 (a): occupancies of the natural orbitals obtained by diagonalizing the single-particle correlation matrix $M_{\alpha\beta}=\sum_{\sigma}\langle C^{\dagger}_{\alpha\sigma}C_{\beta\sigma}\rangle$, with $C^{\dagger}=\{d^{\dagger},p^{\dagger}_x,p^{\dagger}_y\}$. The natural orbital states/occupancies correspond to the eigenvectors/eigenvalues of $M_{\alpha\beta}$. The inset is a zoom-in of the region that shows a sharp drop at the second band beyond which occupancies are limited (< 2%). (b) and (c): Cu-centered Wannier functions at two different locations constructed from the natural orbitals of the first band. Color/area of the circles indicate the sign/magnitude of the local orbital component. (e): overlap of Wannier functions (truncated to a 5×5 CuO_2 unit cell) with their centers shifted to the same site, showing they are almost translational invariant.

where t_{pd}/t_{pp} hops a hole between nearest-neighbor Cu-O/O-O sites, and the summation $\langle ij\rangle/\langle\langle ij\rangle\rangle$ runs over all relevant pairs of sites. We have chosen a gauge for the orbitals as shown in Fig. 1(a) so that all hoppings are negative; U_d and U_p are the on-site repulsion term on the Cu and O sites; $\Delta_{pd}{=}\epsilon_p-\epsilon_d$ is the energy difference for occupying an O site compared to occupying a Cu site. We set the energy scale with $t_{pd}=1.0$, and take $t_{pp}=0.5$, $U_d=6.0$, $U_p=3.0$, and $\Delta_{pd}=3.5$, unless otherwise noted, which appropriately describes a charge-transfer system where $U_d>\Delta_{pd}$ and $\Delta_{pd}>2t_{pd}$. Estimates for t_{pd} range from 1.1eV [66] to 1.5eV [67]. Comparing with previously used parameters [21, 67], here we increase Δ_{pd} to incorporate the effect of V_{pd}, and choose a somewhat smaller U_d for a stronger pairing response [68]. Systems **h1** and **e1** have hole and electron dopings of 0.15. Another hole-doped case **h2** with U_d=3.5 and Δ_{pd}=5.0 describes a Mott-Hubbard rather than charge-transfer system [69]. The calculations are carried out using the `ITensor` library [70]. We typically perform around 20 sweeps and keep a maximum bond dimension of 7000 to ensure convergence with a maximum truncation error of $\mathcal{O}(10^{-5})$.

Previous studies of the three-band model have identified features consistent with the cuprates, including doping asymmetry, formation of stripes on the hole doped side and commensurate AFM on the electron-doped side [20, 21]. There is evidence for d-wave pairing for both electron and hole doping, with the dominant component between nearest neighbor Cu sites [18, 19, 23, 71, 72].

Of particular concern for finite size effects is the quantization of stripe filling around a short cylinder [21]; here we choose a width-5 cylinder so that one stripe can form lengthwise; see Fig. 1(b). The Cu-Cu pairing is shown in Fig. 1(e). Along the stripe an additional pairing modulation reflects an edge-induced charge density oscillation, as shown in Fig. 1(c). Similar pairing occurs whether it is pinned by edge pair fields [Fig. 1(d)] or allowed to arise spontaneously as a finite bond dimension broken symmetry [2] [Fig. 1(e)]. The existance of pairing for a hole-doped three-band model has also been reported in a recent infinite projected entangled-pair states study [73].

Downfolding into a Wannier single-band model.—The occupied bands in the DMRG wavefunctions are identified by measuring the single-particle correlation matrix $M_{\alpha\beta}=\sum_{\sigma}\langle C^{\dagger}_{\alpha\sigma}C_{\beta\sigma}\rangle$, with $\{C^{\dagger}\}=\{d^{\dagger},p^{\dagger}_x,p^{\dagger}_y\}$, whose eigenvectors and eigenvalues define the natural orbitals (NOs) and their occupancies, respectively. In a non-interacting system, the NO occupancies make a step function at the Fermi level. Here, this step near $i\sim 35$ is completely smeared out [Fig. 2(a)], reflecting the strong correlation in the system. However, there is a sharp drop in occupancies at $i=60$, the total number of Cu sites, indicating the end of the first band. Beyond the first band, the total occupancy is $< 2\%$, and for the electron doped case, $< 0.4\%$. This provides a strong justification for downfolding into a single-band, which would be exact if the higher-band occupancies were zero. We observe similar sharp drop-offs for narrower width 2 and 4 systems. This indicates that the drop-off is due to short-range physics involving the Cu and surrounding O orbitals, which can be seen clearly on small systems. We observe a similar sharp drop-off for a range of three-band parameters, including in the Mott-Hubbard regime.

Given the accuracy of the truncation to a single band, we can derive an effective single-band model through the standard Wannier construction with a simple single-particle transformation. We first localize the functions of this band into Cu-centered Wannier functions (WFs), see Ref. [68] for details. We show two representative WFs in Fig. 2(b) and (c), which are evidently highly localized. Functions on different sites are almost identical; evidence for this translational invariance is shown in Fig. 2(d).

To construct the effective Hamiltonian in the WF space, we first organize the WFs into a $N_{\rm Cu}$-by-($N_{\rm Cu} + N_{\rm O}$) real isometric matrix $\mathbf{A}$ ($\mathbf{A}\mathbf{A}^\dagger{=}\mathbb{1}$) , with entry A_{ij} being the weight of the three-band orbital j in the Wannier function centered at Cu site i [74]. The matrix $\mathbf{A}$ defines a single-particle transformation from the three-band basis $\{C^\dagger\} = \{d^\dagger, p_x^\dagger, p_y^\dagger\}$ to the WF basis $\{c^\dagger\}$:

$$c_i^\dagger = \sum_j A_{ij} C_j^\dagger \tag{2}$$

We invert this relationship, taking:

$$C_j^\dagger = \sum_i A_{ij} c_i^\dagger + \text{higher bands} \tag{3}$$

where we omit the higher bands. The Wannier Hamiltonian is obtained by inserting Eq. 3 into the three-band Hamiltonian [Eq. 1]. The single-particle terms $k_{\alpha\beta}$, which include the t_{pd}, t_{pp} and Δ_{pd} terms, become

$$k_{\alpha\beta} C_{\alpha\sigma}^\dagger C_{\beta\sigma} \to k_{\alpha\beta} \sum_{ij} A_{i\alpha} A_{j\beta}\ c_{i\sigma}^\dagger c_{j\sigma}. \tag{4}$$

The two-particle terms U_α, which include the U_d and U_p terms, become

$$U_\alpha n_{\alpha\uparrow} n_{\alpha\downarrow} \to U_\alpha \sum_{ijkl} A_{i\alpha} A_{j\alpha} A_{k\alpha} A_{l\alpha}\ c_{i\uparrow}^\dagger c_{j\uparrow}\ c_{k\downarrow}^\dagger c_{l\downarrow}. \tag{5}$$

Although the Wannier Hamiltonian has $\mathcal{O}(N^2)$ single particle and $\mathcal{O}(N^4)$ two particle terms, both the single-particle and two-particle terms decay quickly with the distance between sites. Magnitudes of the single-particle hoppings beyond third-nearest neighbors are smaller than $0.01t$ and are truncated. The largest two-particle term is the onsite repulsion U. The second largest is the nearest-neighbor density-assisted hopping $t_n c_{j,\sigma}^\dagger c_{i,\sigma} n_{i\bar\sigma}$. We also keep the second and third nearest-neighbor density-assisted hoppings (t_n' and t_n''). All other two-particle terms are less than $0.05t$ and are truncated. After these simplifications, we obtain a *truncated Wannier model*:

$$\begin{aligned} H = &\sum_{i,\delta,\sigma} -t^\delta c_{i+\delta,\sigma}^\dagger c_{i,\sigma} + \sum_i U n_{i,\uparrow} n_{i,\downarrow} \\ &+ \sum_{i,\delta_i,\sigma} -t_n^\delta (c_{i+\delta,\sigma}^\dagger c_{i,\sigma} + c_{i,\sigma}^\dagger c_{i+\delta,\sigma}) n_{i\bar\sigma}. \end{aligned} \tag{6}$$

Here $i+\delta$ is the first, second, or third nearest neighbor of site i, with conventional hopping amplitudes t, t', and t'', and with density-assisted hopping amplitudes t_n, t_n', t_n''. The resulting model parameters are summarized in Table. I for downfolding based on three different three-band systems [75].

TABLE I. Parameters for the Wannier single-band model from downfolding the three-band model. **h** and **e** correspond to hole and electron doping of 0.15. t_{pd} is nominally 1.5eV.

case (U_d, Δ_{pd})	t/t_{pd}	t_n/t	t'/t	t_n'/t	t''/t	t_n''/t	U/t
h1 (6.0, 3.5)	0.27	0.60	0.07	0.05	-0.04	-0.09	12.6
e1 (6.0, 3.5)	0.28	0.52	0.08	0.08	-0.05	-0.04	13.7
h2 (3.5, 5.0)	0.21	0.33	0.08	0.05	-0.03	-0.04	11.8

Note that the nearest-neighbor t_n coefficients are almost twice the size of an effective exchange coupling $J \sim 4t^2/U \sim 0.32$. Given their substantial magnitude, it is surprising how rarely these terms have been considered [76–79]. The existance of the t_n term is guaranteed by a finite component of the nearest-neighbor Cu orbitals in the Wannier function, which is robust since regular Wannier functions must have those components to satisfy orthogonality. Its magnitude is substantial mainly because of the large value of U_d. The t_n term is much larger for the cuprate-relevant charge-transfer case **h1**, compared with the Mott-Hubbard case **h2** that has a similar U/t ratio. This is directly tied to the higher O-occupancy in the charge-transfer case, which makes the WFs more extended.

We also note that the WFs and thus the model parameters are similar for the hole and electron doped cases, even if their parental three-band states are quite different in spin and charge order, indicating that the downfolding is determined by the local physics. Just as the sharp drop in occupancy after the first band shows little dependence on system size, we find the Wannier Hamiltonian also exhibits little dependence on cluster size.

Two key questions now arise: (1) does the Wannier model Hamiltonian give the same properties as the three band model? Given the straightforward and robust nature of our downfolding, we expect this to be so, and comparisons detailed in the Supplementary Material [68] for moderate system sizes support this. (2) Does a mean-field treatment of the t_n terms, reducing the system to

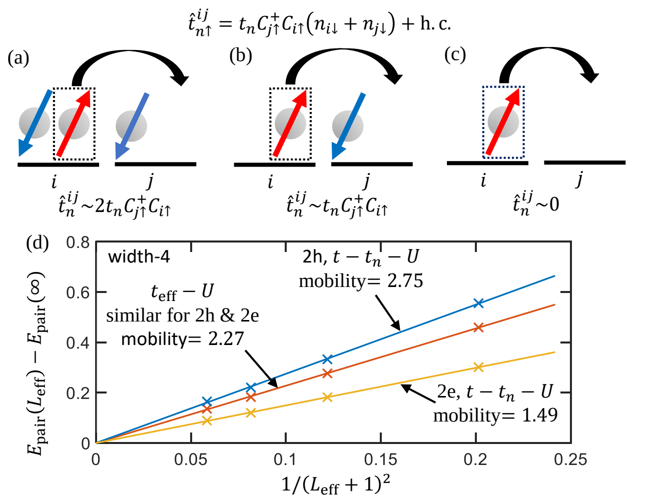

FIG. 3. (a),(b) and (c): action of the t_n term, and resulting hopping strengths, depending on the occupations of the sites involved. (d) On a width-4 cylinder, mobility of a pair of holes/electrons (in unit of t) measured by the slope of pair energy versus $1/(L_{\text{eff}}+1)^2$, for the t-t_n-U model and the t_{eff}-U model.

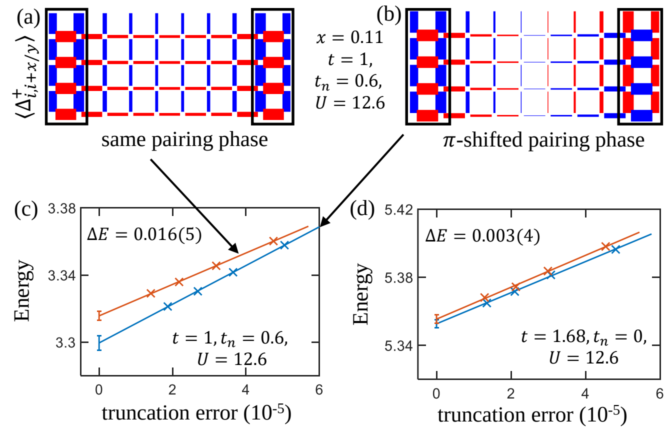

FIG. 4. Pairing response for the t-t_n-U model in a 10×4 cylinder at a hole doping $\sim 0.11 (n \approx 1.11)$. Pair-fields have been applied to regions near both edges, denoted by the black boxes, with the phases on the two ends (a) being the same and (b) having a π shift. (c): extrapolation of the energies with the truncation errors for the two different pairfield boundary conditions in (a) and (b). The energy difference is a measurement of the superconducting phase stiffness. (d) Same as (c) for the t_{eff}-U model that incorporates the effect of the t_n term only in mean-field.

a standard Hubbard model, also match the properties of the three-band model? Although this may be largely true for the spin and charge degrees of freedom, we will argue that the delicate nature of the pairing is not correctly captured by the mean field/standard Hubbard treatment. In any case, the large magnitude of t_n poses a potential difficulty for a mean-field treatment since any deviations could be significant.

Effects of t_n—We find that the t_n terms have two primary effects: first, they reduce the effective interaction strength U/t_{eff}; and second, they enhance hole hopping, reducing the effective mass of pairs on the hole-doped side and promoting phase coherence. The reduction of U/t_{eff} can be understood from a mean-field treatment of t_n where one replaces $t_n c^\dagger_{j\sigma} c_{i\sigma}(n_{i\bar{\sigma}} + n_{j\bar{\sigma}})$ by $t_n c^\dagger_{j\sigma} c_{i\sigma}\langle n\rangle$, with $\langle n\rangle$ being the average density of holes per Cu site, adding to the conventional hopping. This changes $U/t \sim 13$ to $U/t_{\text{eff}} \sim 7.5$ (for t_n=0.6, n=1.15), close to $U/t = 8$, which is often used for the cuprates.

Beyond mean-field, we consider specific hopping processes in Fig. 3(a-c), written in the hole-picture. For a doped hole (i.e. a doublon) we expect process (a) to be relevant, where the t_n acts with magnitude $2t_n$. For undoped regions with AF particle-hole virtual hoppings, process (b) acts with magnitude t_n. On the electron doped side, process (c), t_n has no effect. It does not seem possible to capture these various properties correctly with a mean field treatment.

We find that the resulting hole-pair mobility is enhanced with the $t_n c^\dagger_{j,\sigma} c_{i,\sigma} n_{i\bar{\sigma}}$ term versus its mean-field $t_n c^\dagger_{j,\sigma} c_{i,\sigma}\langle n_{i\bar{\sigma}}\rangle$, $2.75t$ versus $2.27t$. In contrast, the mobility of a pair of electrons with t_n is much smaller, $1.49t$, and reduced comparing to its mean-field $2.27t$. Thus, the increased mobility of a single pair hints at the possibility of enhanced pairing due to t_n on the hole doped side.

To probe for superconductivity, we apply edge pair-fields to a 10×4 cylinder with and without a π phase shift between the two edges, to measure the superconducting phase stiffness α. The results are shown in Fig. 4. Note that $\alpha = 0$ indicates the absence of superconductivity. The applied fields make α proportional to an energy difference, $\alpha \propto \frac{L_x}{L_y}\Delta E$, where ΔE can be extrapolated using DMRG. At a hole doping of 0.11 ($\langle n\rangle \approx 1.11$), the t-t_n-U model gives a stiffness α that is five times larger than the t_{eff}-U model [80]. The pure Hubbard model (without t' terms) is thought to be non-superconducting [1]; our results hint that the t_n terms, even without t', might tip the balance towards superconductivity. In a more realistic model where t' and t'_n from Table. I are included, we also find a larger phase stiffness, $\Delta E = 0.012(4)$ with t_n versus $0.002(4)$ with t_{eff}, for a system at a hole doping of 0.11.

Summary and discussion.— We have revisited the Zhang-Rice downfolding of the three-band Hubbard model to a single-band model, basing the downfolding on a DMRG simulation of the three band model. Our results give strong support to the applicability of the one band approach, where the small occupancy of higher natural orbital bands shows their irrelevance. However, our Wannier function downfolding also shows that a density-assisted hopping term which is usually neglected has a large coefficient. This term renormalizes the hopping in mean field, but mean field treatments are inadequate to capture the effects of this term on pairing. The density-assisted hopping enhances hole mobility and hole-pair mobility. This leads to enhanced superconducting pairing on the hole-doped side on width-4 cylinders.

Acknowledgments.— We acknowledge helpful discussion with A. Georges, H.-C. Jiang, S. Sondhi and S. A. Kivelson. SJ and SRW are supported by the NSF under DMR-2110041.

* shengtaj@uci.edu

[1] M. Qin, C.-M. Chung, H. Shi, E. Vitali, C. Hubig, U. Schollwöck, S. R. White, and S. Zhang (Simons Collaboration on the Many-Electron Problem), Absence of superconductivity in the pure two-dimensional Hubbard model, Phys. Rev. X **10**, 031016 (2020).

[2] S. Jiang, D. J. Scalapino, and S. R. White, Ground-state phase diagram of the t-t'-J model, Proc. Natl. Acad. Sci. U.S.A. **118** (2021).

[3] S. Gong, W. Zhu, and D. N. Sheng, Robust d-wave superconductivity in the square-lattice t-J model, Phys. Rev. Lett. **127**, 097003 (2021).

[4] H.-C. Jiang and S. A. Kivelson, High temperature superconductivity in a lightly doped quantum spin liquid, Phys. Rev. Lett. **127**, 097002 (2021).

[5] H.-C. Jiang, S. A. Kivelson, and D.-H. Lee, Superconducting valence bond fluid in lightly doped 8-leg t-J cylinders, arXiv:2302.11633 (2023).

[6] X. Lu, F. Chen, W. Zhu, D. N. Sheng, and S.-S. Gong, Emergent Superconductivity and Competing Charge Orders in Hole-Doped Square-Lattice t-J Model, arXiv:2304.03963 (2023).

[7] Y.-F. Jiang, T. P. Devereaux, and H.-C. Jiang, Ground state phase diagram and superconductivity of the doped Hubbard model on six-leg square cylinders, arXiv:2303.15541 (2023).

[8] H. Xu, C.-M. Chung, M. Qin, U. Schollwöck, S. R. White, and S. Zhang, Coexistance of superconductivity with partially filled stripes in the Hubbard model, arXiv:2303.08376 (2023).

[9] E. W. Huang, T. Liu, W. O. Wang, H.-C. Jiang, P. Mai, T. A. Maier, S. Johnston, B. Moritz, and T. P. Devereaux, Fluctuating intertwined stripes in the strange metal regime of the Hubbard model, arXiv:2202.08845 (2022).

[10] P. Mai, S. Karakuzu, G. Balduzzi, S. Johnston, and T. A. Maier, Intertwined spin, charge, and pair correlations in the two-dimensional Hubbard model in the thermodynamic limit, Proc. Natl. Acad. Sci. U.S.A. **119**, e2112806119 (2022).

[11] S. Jiang, D. J. Scalapino, and S. R. White, Pairing properties of the t-t'-t''-J model, Phys. Rev. B **106**, 174507 (2022).

[12] M. Qin, T. Schäfer, S. Andergassen, P. Corboz, and E. Gull, The Hubbard model: A Computational Perspective, Annu. Rev. Condens. Matter Phys. **13**, 275 (2022).

[13] W. He, J. Wen, H.-C. Jiang, G. Xu, W. Tian, T. Taniguchi, Y. Ikeda, M. Fujita, and Y. S. Lee, Prevalence of tilted stripes in $La_{1.88}Sr_{0.12}Cuo_4$ and the importance of t' in the Hamiltonian, arXiv:2107.10264 (2021).

[14] E. W. Huang, C. B. Mendl, H.-C. Jiang, B. Moritz, and T. P. Devereaux, Stripe order from the perspective of the Hubbard model, npj Quantum Mater. **3**, 1 (2018).

[15] S. Karakuzu, A. Tanjaroon Ly, P. Mai, J. Neuhaus, T. A. Maier, and S. Johnston, Stripe correlations in the two-dimensional Hubbard-Holstein model, Commun. Phys. **5**, 1 (2022).

[16] V. J. Emery, Theory of high-T_c superconductivity in oxides, Phys. Rev. Lett. **58**, 2794 (1987).

[17] E. W. Huang, C. B. Mendl, S. Liu, S. Johnston, H.-C. Jiang, B. Moritz, and T. P. Devereaux, Numerical evidence of fluctuating stripes in the normal state of high-T_c cuprate superconductors, Science **358**, 1161 (2017).

[18] P. Mai, G. Balduzzi, S. Johnston, and T. A. Maier, Orbital structure of the effective pairing interaction in the high-temperature superconducting cuprates, npj Quantum Mater. **6**, 1 (2021).

[19] Z.-H. Cui, C. Sun, U. Ray, B.-X. Zheng, Q. Sun, and G. K.-L. Chan, Ground-state phase diagram of the three-band hubbard model from density matrix embedding theory, Phys. Rev. Res. **2**, 043259 (2020).

[20] A. Chiciak, E. Vitali, and S. Zhang, Magnetic and charge orders in the ground state of the Emery model: Accurate numerical results, Phys. Rev. B **102**, 214512 (2020).

[21] S. R. White and D. J. Scalapino, Doping asymmetry and striping in a three-orbital CuO_2 Hubbard model, Phys. Rev. B **92**, 205112 (2015).

[22] N. Kowalski, S. S. Dash, P. Sémon, D. Sénéchal, and A.-M. Tremblay, Oxygen hole content, charge-transfer gap, covalency, and cuprate superconductivity, Proc. Natl. Acad. Sci. U.S.A. **118**, e2106476118 (2021).

[23] A. Biborski, M. Zegrodnik, and J. Spałek, Superconducting properties of the hole-doped three-band $d-p$ model studied with minimal-size real-space d-wave pairing operators, Phys. Rev. B **101**, 214504 (2020).

[24] S. Li, A. Nocera, U. Kumar, and S. Johnston, Particle-hole asymmetry in the dynamical spin and charge responses of corner-shared 1d cuprates, Commun. Phys. **4**, 217 (2021).

[25] F. C. Zhang and T. M. Rice, Effective Hamiltonian for the superconducting Cu oxides, Phys. Rev. B **37**, 3759 (1988).

[26] N. B. Brookes, G. Ghiringhelli, O. Tjernberg, L. H. Tjeng, T. Mizokawa, T. W. Li, and A. A. Menovsky, Detection of Zhang-Rice Singlets Using Spin-Polarized Photoemission, Phys. Rev. Lett. **87**, 237003 (2001).

[27] L. H. Tjeng, B. Sinkovic, N. B. Brookes, J. B. Goedkoop, R. Hesper, E. Pellegrin, F. M. F. de Groot, S. Altieri, S. L. Hulbert, E. Shekel, and G. A. Sawatzky, Spin-Resolved Photoemission on Anti-Ferromagnets: Direct Observation of Zhang-Rice Singlets in CuO, Phys. Rev. Lett. **78**, 1126 (1997).

[28] Y. Harada, K. Okada, R. Eguchi, A. Kotani, H. Takagi, T. Takeuchi, and S. Shin, Unique identification of Zhang-Rice singlet excitation in $Sr_2CuO_2Cl_2$ mediated by the O $1s$ core hole: Symmetry-selective resonant soft x-ray Raman scattering study, Phys. Rev. B **66**, 165104 (2002).

[29] E. Arrigoni, M. Aichhorn, M. Daghofer, and W. Hanke, Phase diagram and single-particle spectrum of CuO_2 high-T_c layers: variational cluster approach to the three-band Hubbard model, New J. Phys. **11**, 055066 (2009).

[30] I. J. Hamad, L. O. Manuel, and A. A. Aligia, Generalized One-Band Model Based on Zhang-Rice Singlets for Tetragonal CuO, Phys. Rev. Lett. **120**, 177001 (2018).

[31] V. Marino, F. Becca, and L. F. Tocchio, Stripes in the extended $t-t'$ Hubbard model: A Variational Monte Carlo analysis, SciPost Phys. **12**, 180 (2022).

[32] Y.-F. Jiang, J. Zaanen, T. P. Devereaux, and H.-C. Jiang, Ground state phase diagram of the doped Hubbard model on the four-leg cylinder, Phys. Rev. Research **2**, 033073 (2020).

[33] K. Ido, T. Ohgoe, and M. Imada, Competition among various charge-inhomogeneous states and d-wave superconducting state in Hubbard models on square lattices, Phys. Rev. B **97**, 045138 (2018).

[34] L. F. Tocchio, F. Becca, and S. Sorella, Hidden Mott transition and large-U superconductivity in the two-dimensional Hubbard model, Phys. Rev. B **94**, 195126 (2016).

[35] S. Sorella, The phase diagram of the Hubbard model by variational auxiliary field quantum monte carlo (2021), arXiv:2101.07045.

[36] K. Ido, T. Ohgoe, and M. Imada, Competition among various charge-inhomogeneous states and d-wave superconducting state in Hubbard models on square lattices, Phys. Rev. B **97**, 045138 (2018).

[37] L. F. Tocchio, A. Montorsi, and F. Becca, Metallic and insulating stripes and their relation with superconductivity in the doped Hubbard model, SciPost Phys. **7**, 21 (2019).

[38] D. Sénéchal, P.-L. Lavertu, M.-A. Marois, and A.-M. S. Tremblay, Competition between antiferromagnetism and superconductivity in high-T_c cuprates, Phys. Rev. Lett. **94**, 156404 (2005).

[39] K. Machida, Magnetism in La_2CuO_4 based compounds, Physica C Supercond. **158**, 192 (1989).

[40] X. Y. Xu and T. Grover, Competing nodal d-wave superconductivity and antiferromagnetism, Phys. Rev. Lett. **126**, 217002 (2021).

[41] A. Himeda, T. Kato, and M. Ogata, Stripe states with spatially oscillating d-wave superconductivity in the two-dimensional $t-t'-J$ model, Phys. Rev. Lett. **88**, 117001 (2002).

[42] H.-C. Jiang and S. A. Kivelson, Stripe order enhanced superconductivity in the hubbard model, Proc. Natl. Acad. Sci. U.S.A. **119**, e2109406119 (2022).

[43] H. Xu, H. Shi, E. Vitali, M. Qin, and S. Zhang, Stripes and spin-density waves in the doped two-dimensional hubbard model: Ground state phase diagram, Phys. Rev. Res. **4**, 013239 (2022).

[44] J. P. F. LeBlanc, A. E. Antipov, F. Becca, I. W. Bulik, G. K.-L. Chan, C.-M. Chung, Y. Deng, M. Ferrero, T. M. Henderson, C. A. Jiménez-Hoyos, E. Kozik, X.-W. Liu, A. J. Millis, N. V. Prokof'ev, M. Qin, G. E. Scuseria, H. Shi, B. V. Svistunov, L. F. Tocchio, I. S. Tupitsyn, S. R. White, S. Zhang, B.-X. Zheng, Z. Zhu, and E. Gull (Simons Collaboration on the Many-Electron Problem), Solutions of the two-dimensional Hubbard model: Benchmarks and results from a wide range of numerical algorithms, Phys. Rev. X **5**, 041041 (2015).

[45] B.-X. Zheng, C.-M. Chung, P. Corboz, G. Ehlers, M.-P. Qin, R. M. Noack, H. Shi, S. R. White, S. Zhang, and G. K.-L. Chan, Stripe order in the underdoped region of the two-dimensional hubbard model, Science **358**, 1155 (2017).

[46] C. Peng, Y. Wang, J. Wen, Y. Lee, T. Devereaux, and H.-C. Jiang, Enhanced superconductivity by near-neighbor attraction in the doped Hubbard model, arXiv:2206.03486 (2022).

[47] A. Wietek, Y.-Y. He, S. R. White, A. Georges, and E. M. Stoudenmire, Stripes, antiferromagnetism, and the pseudogap in the doped Hubbard model at finite temperature, Phys. Rev. X **11**, 031007 (2021).

[48] S. Raghu, S. A. Kivelson, and D. J. Scalapino, Superconductivity in the repulsive Hubbard model: An asymptotically exact weak-coupling solution, Phys. Rev. B **81**, 224505 (2010).

[49] B. Xiao, Y.-Y. He, A. Georges, and S. Zhang, Temperature Dependence of Spin and Charge Orders in the Doped Two-Dimensional Hubbard Model, Phys. Rev. X **13**, 011007 (2023).

[50] M. Danilov, E. G. van Loon, S. Brener, S. Iskakov, M. I. Katsnelson, and A. I. Lichtenstein, Degenerate plaquette physics as key ingredient of high-temperature superconductivity in cuprates, npj Quantum Mater. **7**, 50 (2022).

[51] P. Corboz, T. M. Rice, and M. Troyer, Competing states in the $t-J$ model: Uniform d-wave state versus stripe state, Phys. Rev. Lett. **113**, 046402 (2014).

[52] H.-C. Jiang, Z.-Y. Weng, and S. A. Kivelson, Superconductivity in the doped $t-J$ model: Results for four-leg cylinders, Phys. Rev. B **98**, 140505(R) (2018).

[53] J. F. Dodaro, H.-C. Jiang, and S. A. Kivelson, Intertwined order in a frustrated four-leg $t-J$ cylinder, Phys. Rev. B **95**, 155116 (2017).

[54] P. Corboz, S. R. White, G. Vidal, and M. Troyer, Stripes in the two-dimensional t-J model with infinite projected entangled-pair states, Phys. Rev. B **84**, 041108(R) (2011).

[55] C.-P. Chou and T.-K. Lee, Mechanism of formation of half-doped stripes in underdoped cuprates, Phys. Rev. B **81**, 060503(R) (2010).

[56] W.-C. Chen, Y. Wang, and C.-C. Chen, Superconducting Phases of the Square-Lattice Extended Hubbard Model, arXiv:2206.01119 (2022).

[57] D.-W. Qu, B.-B. Chen, X. Lu, Q. Li, Y. Qi, S.-S. Gong, W. Li, and G. Su, d-wave superconductivity, pseudogap, and the phase diagram of t-t'-J model at finite temperature (2022).

[58] X. Lu, D.-W. Qu, Y. Qi, W. Li, and S.-S. Gong, Ground-state phase diagram of the extended two-leg $t-J$ ladder, Phys. Rev. B **107**, 125114 (2023).

[59] S. R. White, Density matrix formulation for quantum renormalization groups, Phys. Rev. Lett. **69**, 2863 (1992).

[60] Y. Chang and L. K. Wagner, Learning emergent models from *ab initio* many-body calculations, arXiv:2302.02899 (2023).

[61] H. J. Changlani, H. Zheng, and L. K. Wagner, Density-matrix based determination of low-energy model hamiltonians from ab initio wavefunctions, J. Chem. Phys. **143**, 102814 (2015).

[62] Z.-H. Cui, H. Zhai, X. Zhang, and G. K.-L. Chan, Systematic electronic structure in the cuprate parent state from quantum many-body simulations, Science **377**, 1192 (2022).

[63] H. Zheng, H. J. Changlani, K. T. Williams, B. Busemeyer, and L. K. Wagner, From real materials to model hamiltonians with density matrix downfolding, Front. Phys. **6**, 10.3389/fphy.2018.00043 (2018).

[64] M. Hirayama, Y. Nomura, and R. Arita, Ab Initio Downfolding Based on the GW Approximation for Infinite-Layer Nickelates, Front. Phys. , 49 (2022).

[65] R. C. Sawaya and S. R. White, Constructing Hubbard models for the hydrogen chain using sliced-basis density matrix renormalization group, Phys. Rev. B **105**, 045145 (2022).

[66] Y. F. Kung, C.-C. Chen, Y. Wang, E. W. Huang, E. A. Nowadnick, B. Moritz, R. T. Scalettar, S. Johnston, and T. P. Devereaux, Characterizing the three-orbital Hubbard model with determinant quantum Monte Carlo, Phys. Rev. B **93**, 155166 (2016).

[67] W. Hanke, M. L. Kiesel, M. Aichhorn, S. Brehm, and E. Arrigoni, The 3-band Hubbard-model versus the 1-band model for the high-T_c cuprates: Pairing dynamics, superconductivity and the ground-state phase diagram, Eur. Phys. J.: Spec. Top. **188**, 15 (2010).

[68] See Supplemental Material at [], which includes Refs. [19, 65, 67, 81],for the parameters choice for the three-band Hubbard model, details of constructing Wannier functions and further calculations of the Wannier single-band model.

[69] See Ref.[82] for detailed definitions of a charge-transfer insulator and Mott-Hubbard insulator.

[70] M. Fishman, S. R. White, and E. M. Stoudenmire, The ITensor Software Library for Tensor Network Calculations, SciPost Phys. Codebases , 4 (2022).

[71] H.-C. Jiang, Pair density wave in doped three-band Hubbard model on square lattice, arXiv:2209.11381 (2022).

[72] J.-P. Song, S. Mazumdar, and R. T. Clay, Absence of Luther-Emery superconducting phase in the three-band model for cuprate ladders, Phys. Rev. B **104**, 104504 (2021).

[73] B. Ponsioen, S. S. Chung, and P. Corboz, Superconducting stripes in the hole-doped three-band Hubbard model, arXiv:2306.12910 (2023).

[74] The matrix elements of **A** are listed in Ref. [68] Sec.II.

[75] The hopping coefficients are averaged over horizontal and vertical directions, which typically differ by $\sim 10\%$, but somewhat more (-0.07 and -0.11) in the case of t_n'' in system **h1**.

[76] F. Werner, O. Parcollet, A. Georges, and S. R. Hassan, Interaction-induced adiabatic cooling and antiferromagnetism of cold fermions in optical lattices, Phys. Rev. Lett. **95**, 056401 (2005).

[77] J. Hirsch, Bond-charge repulsion and hole superconductivity, Phys. C: Supercond. Appl. **158**, 326 (1989).

[78] R. B. Laughlin, Fermi-liquid computation of the phase diagram of high-T_c cuprate superconductors with an orbital antiferromagnetic pseudogap, Phys. Rev. Lett. **112**, 017004 (2014).

[79] S. L. Sondhi, M. P. Gelfand, H. Q. Lin, and D. K. Campbell, Off-diagonal interactions, Hund's rules, and pair binding in c_{60}, Phys. Rev. B **51**, 5943 (1995).

[80] In the supplementary material [68], we vary t_n from 0 to 1.6 and find that the superconducting phase stiffness gets bigger as t_n increases, and the phase stiffness is greater compared to using a mean-field t_{eff}.

[81] P.-O. Löwdin, On the non-orthogonality problem connected with the use of atomic wave functions in the theory of molecules and crystals, J. Chem. Phys. **18**, 365 (1950).

[82] J. Zaanen, G. A. Sawatzky, and J. W. Allen, Band gaps and electronic structure of transition-metal compounds, Phys. Rev. Lett. **55**, 418 (1985).